Laser Welding of Low Alloy Cr-Mo Steel and Ductile Iron

Ing. Petr Vondrouš

Vedoucí práce: prof. Ing. Jiří Dunovský

Abstrakt - CZE

Laserové svařování je velmi produktívní technologií svařování, která navíc umožňuje svařovat i obtížně svařitelné materiály. Tyto a další charakteristiky činí tuto metodu dobře využitelnou pro automobilový průmysl. V pohonném soustrojí automobilů se nachází často kombinace dílů z nízkolegované Cr-Mo oceli a litiny s kuličkovým grafitem. Příspěvek se zaměřuje na možnosti laserového svařování těchto nesourodých materiálů. V příspěvku jsou provedeny experimenty svařitelnosti materiálů jednotlivě i jejich kombinace. Byla zjištěna obtížná svařitelnost obou materiálů, vznik trhlin za studena i za horka. Vytvoření nesourodých svarů bez trhlin bylo dosaženo kontrolou vzájemného poměru promíšení obou materiálů a také použitím přídavného Ni drátu.

Klíčová slova

Laser, svařování, nesourodé materiály, LKG, nízkolegovaná ocel

Abstract - ENG

Laser welding is very progressive technology, that makes feasible welding even of materials with difficult weldability. Characteristics of laser welding make it a great option for automotive industry. For powertrain components often ductile iron and high strength low alloy steel are used. The laser weldability of the materials separately and their combination is researched. Cold cracking, solidification cracking and other weld defects are observed. The high quality dissimilar laser welds were obtained by controlling mixing of the 2 metal in WM by laser misalignment and also using Ni filler wire.

Keywords

Laser, dissimilar materials, welding, ductile iron, low alloy steel

1. Introduction

More and more modern high power and high beam quality laser sources are available at the industrial market. These modern laser sources are in the focus of automotive industry, because they are suitable for deep penetration, high quality and high productivity welding. Nowadays laser welding is good option not only for tailored welded blanks, but also for welding of engine and powertrain components.

The laser beam is a radiation of light with very high beam power density (up to $10^8 W/cm^2$ for welding applications) and specifics of laser beam make the laser welding process very different from standard arc welding processes. Usually the weldability of materials for arc welding is known, but data of laser weldability are not.

Ductile iron and low alloy Cr-Mo steel are materials often used in automotive industry for construction of engine, powertrain components, e.g. gear and shaft, gear and gear case. There is often need to connect these 2 materials and laser welding is considered as the best welding method to substitute screwed connection used nowadays. The experiments of laser dissimilar welding are done because there is big potential of use in the industry. These

materials are subjected to research of dissimilar metal laser weldability, where properties of melt behavior, cracking behavior and so on are observed.

2. Experimental setup

At first two base materials have been subjected to research of laser weldability separately. To research the laser weldability the bead-on-plate (further BOP) welding of materials 1) FCD600 and 2) SCM420 was done.

2.1 Used materials

Both materials, FCD600, SCM420, are using denomination according to japanese JIS norms, because research was conducted in Japan. Their respective equivalents are also stated.

FCD600 is ductile iron (C 3.4 %, Si 2.5 %, other). It has pearlitic-feritic matrix with nodular graphite. The material has high tensile strength, good castability and is often used for castings of pistons, valves, tubes, gears. Equivalent of this material is DIN GGG60.

SCM420 is high strength low alloy Cr-Mo steel (C 0.2 %, Cr 1.1 %, Mo 0.15 %, Mn 0.8 %, other). The matrix is pearlitic-feritic. Material is suitable for heat treatment, has high tensile, fatigue strengths and is used for gears, shafts, pistons and other engine components. The closest material equivalent is DIN 25CrMo4 and SAE 4130.

2.2 Laser source, welding head

Modern disc laser by Trumpf with maximum power 10 kW was used. Laser source properties are in Tab. 1.

Tab. 1 Laser source parameters

Manufacturer	Trumpf
Maximum power	10 kW
Wavelength	1030 nm
BPP	12 mm*rad
Fiber core diameter	0.3 mm

As welding head 2 different welding heads are used.

1. For bead on plate welding (BOP) Trumpf welding head (f=200 mm, spot diameter 0.3 mm) is used.
2. For BOP welding, butt welding and use of filler wire the HighYag welding head (f=250 mm, spot diameter 0.45 mm) with wire feeding possibility is used.

2.3 Welding setup

Laser is connected to welding head by optical fiber. Sample of dimensions 40x150x30 mm is mounted on moving stage that executes the movement. For observation of the welding process 2 high speed cameras have been used. One camera is set up to observe the molten pool, second camera observes the plume. As shielding gas argon is used. X-ray system with high speed video camera was used to

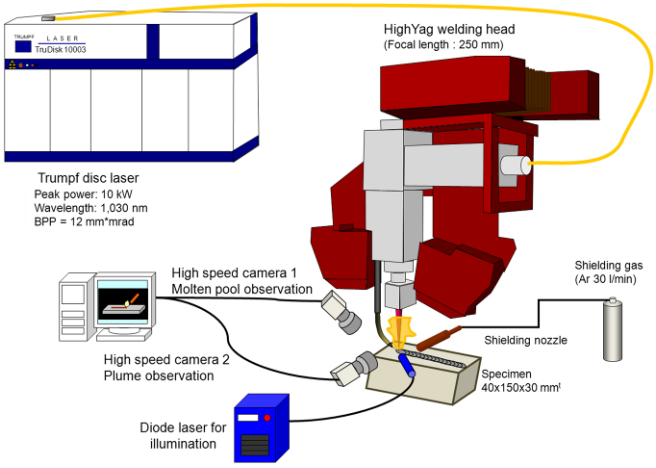

Fig. 1 Welding setup

observe the inner metal flow inside the melt.
The welding setup is on the Fig.1.

2.4 Weld evaluation

The optical metallography was the main method to asses welds` shape and weld quality. To asses weld metal phases, measurement of microhardness and XRD (X-ray diffraction spectroscopy) analysis were used. For fractography SEM was used. For chemical analysis EDS (energy dispersive X-ray spectroscopy) and WDS (wavelength dispersive X-ray spectroscopy) were used.

3. Laser weldability of FCD600

3.1 BOP welding results

At first, variation of welding speed and laser power experiment was done. Laser power was varied 4-10 kW, welding speed varied from 16.67 – 75 mm/s, defocused distance is constant fd=0 mm. Welding head Trumpf is used.

Cross sections are shown at Fig. 2. Welds are very deep and narrow, weld shape ratio (weld depth/ weld width) ranges from 3.5-8.5. Various welding defects are visible. Spatter and subsequent underfill was created resulting in weld shape defect. The severity of spatter and underfill is increasing with welding speed and laser power.

In majority of welds` welding cracks formed. The vertical and perpendicular cracks are observed in WM and HAZ. Weld bead perpendicular cracks are present in all the weld beads.

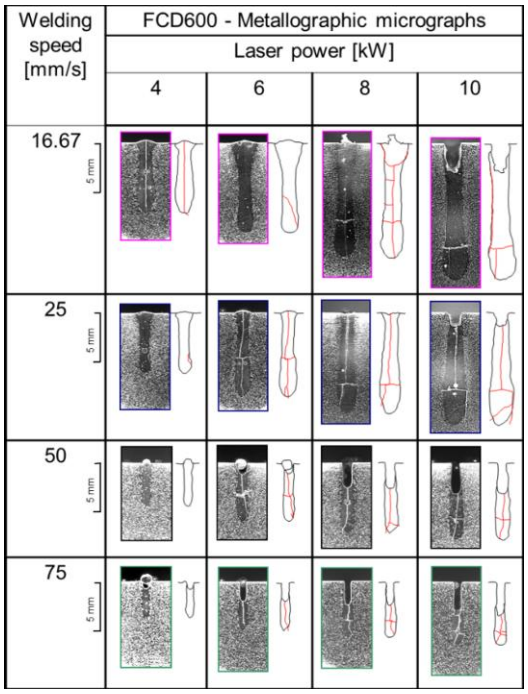

Fig. 2 Cross sections of FCD600, BOP welds

3.2 WM structure, hardness, phases

The typical WM microstructure is shown on fig. 3. The solidification structure of austenite with primary and secondary dendrites is visible. The cementite, martensite needles and plates are visible. Distance of secondary dendritic arms is approximately 2-3 um.

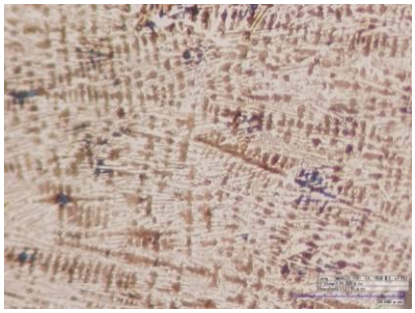

Fig. 3 WM microstructure, 8 kW, 50 mm/s, fd=0 mm, Mag. 1750 x

Tab. 2 Hardness, weld 8 kW, 50mm/s, fd=0 mm

Measured hardness	Maximum	Average
WM hardness	1030 HV1	900 HV1
HAZ hardness	990 HV1	660 HV1
BM hardness	350 HV1	250 HV1

Very high hardness of WM and HAZ compared to BM shows that phase transformations were caused by welding.

The uXRD analysis was used to asses phases present in WM. According to the XRD diffractogram of WM, there is cementite, austenite and martensite present. The austenite phase was found as importan in the WM. Carbon dissolved in austenite has austenite stabilizing properties and with increase of carbon in austenite the martensite start M_s, martensite finish M_f temperature decrease. Exact C volume in matrix was measured by WDS. Average values of C content are listed in Tab. 3. According to graphs C=1.05 % corresponds to M_s=180 °C M_f=-120 °C. [1] So it can be concluded, that presence of retained austenite in WM of FCD600 is because of high C dissolved in matrix. This retained austenite influences the WM properties strongly.

Tab. 3 Carbon content measurement result

Avg. C content	C [%]	Present phases
BM matrix	0.36	Perlite, ferrite
WM matrix	1.05	Cementite, austenite, martensite

3.3 Crack assessment

The weld cracks formed under the majority of the welding conditions as visible on Fig. 2. Cracks run in WM and also HAZ. The fractography observation of cracks was done. In SEM observation of the crack surface, it was found that fracture mode is transcrystalline cleavage fracture, that is typical for brittle materials. The cracks are caused by thermal and phase transformation stresses during fast cooling in combination with presence of brittle cementite, martensite structure in WM. According Fractography Handbook [4] these cracks can be denominated as cracks due to formation of brittle cementite.

From the severity of brittle cracks occurence it can be stated that laser weldability of this material is poor.

4. Laser weldability of SCM420

Experiments noted in chap. 3 done for ductile iron have been also done for Cr-Mo low alloy steel SCM420.

4.1 BOP welding results

Results of variation of laser power and welding speed with const. fd=0 mm are at Fig. 4.

Welds have beam aspect ratio 2.8-10.6. There is a different weld shape for lower and higher welding speed. At 25 mm/s the weld is wider, with lower weld aspect ratio and for speed 50, 75 mm/s the weld is very deep and narrow. Weld shape defects are visible. At high laser power and welding speed, the spatter creation and subsequent underfill is problem. At all cross sections the weld cracks were observed. The cracks usually formed in the lower part of the weld, near the thermal axis and they are obviously different from brittle cracks observed in FCD600.

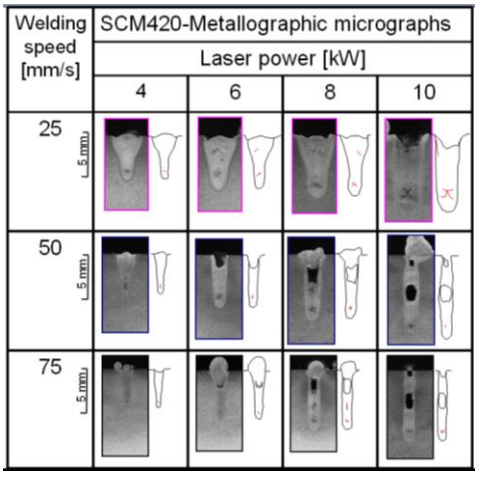

Fig. 4 Cross sections of SCM420, BOP welds

4.2 WM structure, hardness, phases

The typical WM microstructure is shown on Fig. 5. The WM structure is fine grained, consisting from martensitic needles, with length 10-15 um, thickness of 1-2 um. Presence of martensite phase was confirmed by XRD analysis. No other phases were found.

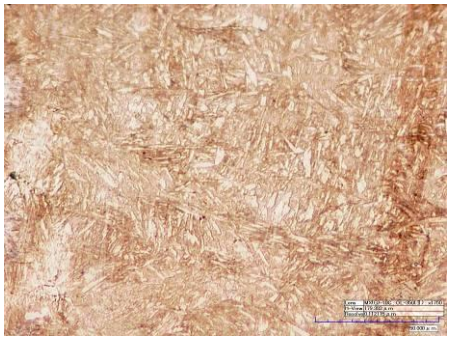

Fig. 5 WM microstructure, 8 kW, 50 mm/s, fd=0 mm, Mag. 1750 x

High measured hardness of WM, Tab. 4, signalizes quenching caused by welding.

Tab. 4 Hardness, weld 8 kW, 50mm/s, fd=0 mm

Measured hardness	Maximum	Average
WM hardness	480 HV1	465 HV1
HAZ hardness	620 HV1	400 HV1
BM hardness	300 HV1	225 HV1

4.3 Crack assessment

In all welded samples weld cracks formed, as visible on Fig. 4. They run only in WM. By fractography analysis, observation in SEM, it was found that fracture surface is dendritic, so it can be said, that cracks in SCM420 are solidification cracks.

Also this material has is poor laser weldability because of formation of solidification cracks.

5. Differences in behavior between 2 materials

As stated in chap. 3, 4, many differences in behavior of ductile iron FCD600 and Cr-Mo steel SCM420 during laser welding under the same welding conditions have been found.

These differences include penetration depth, weld shape, type of occurring cracks, melt behavior, spatter, underfill creation, melt flow directions, melt speed, plume and so on. Mainly physical and chemical properties are considered the cause of this difference.

Both materials have poor laser weldability because of crack formation. In ductile iron brittle cracks due to cementite formation occurs and in Cr Mo low alloy steel solidification cracks form.

6. Dissimilar metal welding

Materials FCD600 and SCM420 have been used for research of dissimilar materials butt laser welding. To achieve dissimilar weld 2 methods are used:

1. Laser beam misalignment
2. Filler wire usage

6.1 Laser beam misalignment

It was considered, that by misalignment of laser beam during butt welding into ductile iron or steel side, the resulting WM structure can be greatly varied. Because chemical composition, mainly level of C content, is very different in both metals, changing the C content in the WM can change greatly phases formed in resulting WM.

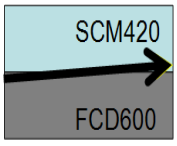

Fig. 6 Misaligned butt welding

6.2 Gradual misalignment

To research influence of gradually changing composition on resulting WM, butt welding under small angle was done. Two

samples are aligned into butt weld and then welding starts inside ductile iron and finishes inside steel part, as on Fig. 6.

For the weld created at 8 kW, 50 mm/s, fd=-2 mm (to suppress spatter), longitudinal cut was prepared and hardness was measured. Results are shown at Fig. 7. It is found that hardness of WM dramatically changes along the longitudinal axis. The hardness ranges between 400–1000 HV. On longitudinal cut it is visible, that in the half way, where the materials mix about half to half, there is decrease of occurring cracks. The part with fewer cracks corresponds with the lowest hardness.

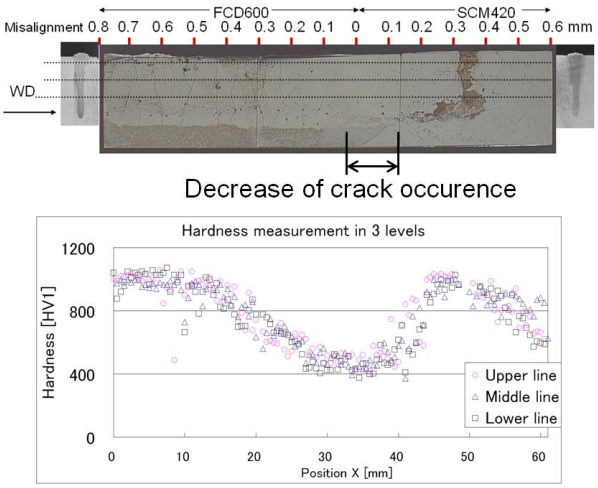

Fig. 7 Longitudinal cut of misaligned weld, hardness measurement along longitudinal axis

The uXRD analysis of phases existent in WM is as follows:

1. Weld beginning - hardness 1000 HV, WM mainly consists of FCD600, little SCM420
   Cementite, Austenite, Martensite
2. Central part – mix of FCD600+SCM420
   Austenite, little martensite+cementite
3. End part – majority of SCM420 + smaller part of FCD600
   Martensite, little austenite

We can notice that the most influential phases are cementite at the weld beginning, than austenite at the weld center and martensite at the end. The formation of dominant phases is closely connected to gradual change of C content in the WM. Carbon content was measured by WDS analysis in respective parts.

1. Eutectic cementite forms mainly at the weld beginning. Approx. 1.4 % C was measured in WM. (Similar to BOP welding of pure FCD600.) Hardness is about 1000 HV.
2. Mixing both metals, overall C content decreases and C is mainly dissolved in austenite. Only little cementite forms and austenite is stabilized in the WM by dissolved C. Measured approx. 1.2-0.6 % C. Hardness was 380-500 HV.
3. Content of C is decreasing further. Approximately 0.6-0.3 % C was measured. This volume of dissolved C is not enough to stabilize austenite upon cooling to room temperature, so martensite transformation. According to C content in austenite, the resulting martensite morphology (plate martensite, lath martensite) and hardness greatly varies (1000-500 HV).

In this experiment it was visible, that cracks occurring in FCD600 and SCM420 are of different nature. At the weld beginning, where cementite forms, cracks due to brittle cementite occur. With decrease of C content, the number and length of cracks due to Fe_3C decreases and vanishes completely, but solidification cracks start to occur at lower part of the weld. Cracks have been found in all the length of the welded sample. At the part of metals mixing half to half decrease of occuring cracks was noticed.

6.3 Constant misalignment

According to the best results of chapter 6.2 the experiments with constant misalignment are done. In butt welding, when austenite was created, also there was decrease of hardness and cracks. To ensure austenite phase creation welds with misalignment 0.15 mm,

0.07 mm into FCD600, no misalignment and misalignment 0.07 mm into SCM420 are created under welding conditions from chapter 6.2. Welding results are at Fig. 8.

As is visible on metallographic photographs there are cracks under all conditions. For misalignment into FCD600 there are also bead perpendicular cracks. With 0 mm, 0.07 mm SCM420 misalignment bead perpendicular cracks are not found, because cementite is almost non present. For the 0.15 mm FCD600 weld, there is crack running at the weld bottom and at the HAZ. In the rest of the welds, solidification cracks occurred at the WM bottom. So it is clear, that with misalignment into ductile iron, brittle cracks would occur and with misalignment into low alloy steel solidification cracks would occur. Hardness of all welds is 385 – 455 HV, structure consists of austenite, martensite and cementite, ratio of these phases changes with misalignment.

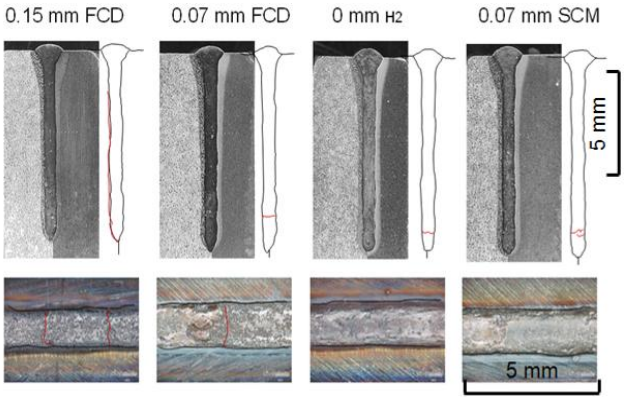

Fig. 8 Metallographic cuts and bead photographs of welds created with constant misalignment

6.4 Suppression of the solidification cracks

It was stated that in constant misalignment butt welds the cracks due to Fe_3C (brittle lateral weld bead cracks, HAZ+WM brittle cracks) and solidification cracks (cracks at the weld bottom) occur. Suppressing of these cracks is of primary importance to create sound welds.

Brittle fracture, cracks due to Fe_3C are caused by thermal stresses and presence of brittle cementite. For suppression of such a cracks it is needed to lower thermal stresses and (or) volume of brittle cementite.

1. To reduce stresses on cooling and to lower the cementite, high preheat is possible. During the BOP welding of FCD600 preheat up to 300 °C was done, but it had no possitive influence on suppresing the cracks. Probably preheat of up to 600 °C would have effect, but it was not possible to reach it in our experiments.
2. The volume of formed cementite in WM is possible to be controled by WM carbon content (misalginment), so misalignment 0 mm, 0.07 mm into SCM420 is enough to suppress cementite formation greatly and successively also brittle cracks.

The solidification cracks are caused by solidification process sequence, solidification stresses and presence of impurities in WM. The process, sequence of solidification and thermal stresses distribution can be greatly influenced by weld shape, so experiments with defocused distance and full penetration welds were done.

During the experiments with defocused distance variation (variation of fd), it was found that high negative defocused distance causes weld with V shape, narrow at the bottom, wider at the top. When weld has V shape, it then complies with an inscribed circle method, known from the foundry industry. Such a shape ensures unidirectional solidification from the weld bottom to the weld top and minimizes the shrinkage stresses. Also the

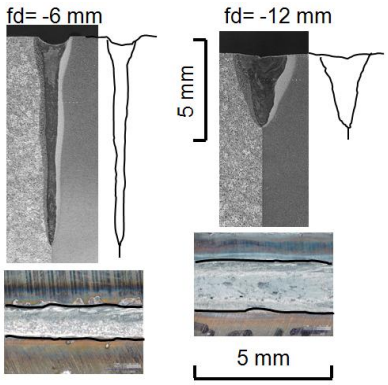

Fig. 9 Metallographic cuts, bead photographs fd= -6, -12 mm

segregation would be better distributed in the weld.

Minus defocused distance experiment

Welds for dissimilar butt welding with 0 mm misalignment were done at 8 kW, 50 mm/s, defocused distance fd=-6 and fd=-12 mm. The cross sections and weld bead photographs are at Fig. 9.

Created welds have V shape and solidified from bottom to top, in unidirectional solidification. No solidification cracks, neither brittle cracks have been found in the metallographic cuts. Neither weld bead perpendicular cracks were found.

Full penetration welds

Partial penetration welds are subjected to higher weld contraction stresses, than full penetration welds, because of weld root opposing to weld shrinkage. [5] To ensure full penetration welds under welding conditions 8 kW, 50 mm/s, 8 mm^t thick samples have been created. On these samples butt welds were created, with and w/o misalignment. The results are at Fig. 10. No cracks have been found in the cross sections, so it can be stated, that full penetration weld is more resistant to solidification cracking and is more suitable than partial penetration welding. At the weld misalignment into FCD600 (0.07 mm FCD), the perpendicular bead cracks have been found, so obviously the brittle cementite is present in the WM structure. In 2 other welds no bead cracks are found.

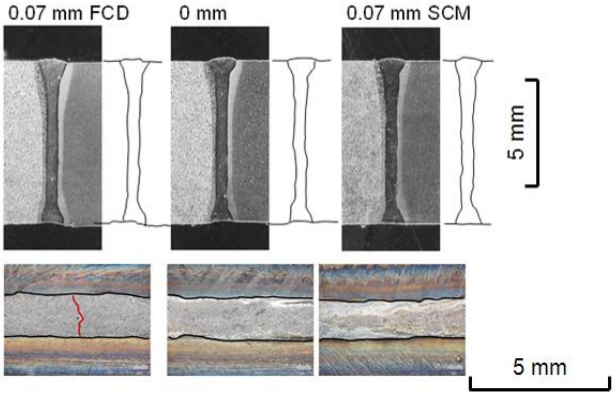

Fig. 10 Full penetration welds, 8 mm^t, with and w/o misalignment, cross sections and weld bead

6.5 Use of Ni filler wire

As the 2nd option to suppress creation of cracks, filler wire was employed. For welding of ductile iron, often Ni based filler wire is used, because carbon is well soluble in Ni and can prevent formation of brittle cementite.

Filler wire ERNi (95 % Ni) and welding head HighYAG equipped with wire feeder were used. Use of filler wire during BOP welding and butt welding with gap=0 mm had shown, that mixing of Ni filler with base metal was inadequate, because Ni did not reach the bottom of the weld and Ni volume was small (0-10 %).

To ensure deeper penetration of

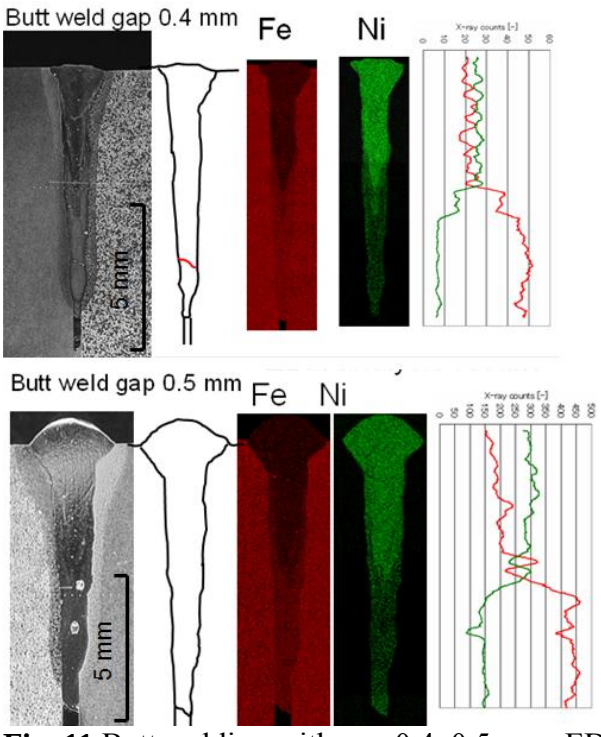

Fig. 11 Butt welding with gap 0.4, 0.5 mm, EDS mapping of Fe, Ni content, line EDS analysis

filler metal within the base metal and to reach higher Ni content in the weld the gap was needed. By gradually increasing the gap the percentage of Ni content in the WM was increasing as in Fig. 11.

As visible on EDS line analysis (Fig. 11, right side) for both examples, the volume of Ni is higher in upper half and much lower in lower half of the weld. With gap 0.4 mm and less the solidification crack were found at the low part of the weld, at position similar to butt welding without filler wire. For gap 0.5 mm, the Ni volume is higher than for gap 0.4 mm, at the upper half of the weld Ni content reaches 60 %, at the bottom part of the weld 35 %. No crack was found for gap 0.5 mm weld. Also for the gap 0.6 mm the sound welds were created.

7. Conclusion

The ductile iron and low alloy Cr-Mo steel were subdued to BOP and dissimilar butt welding to research possibilities of dissimilar metal welding. It can be concluded, that both materials behaviour greatly varies, their laser weldability is poor, but dissimilar material welding is possible.

FCD600 creates very deep welds, with high weld aspect ratio. The creation of spatter is very easy and is causing deep underfill. Ease of spatter creation is caused by welding parameters (power density), strong plume and low surface tension of the material. Resulting WM consist of cementite, retained austenite and martensite. Cracks due to Fe_3C occur in the WM and HAZ.

SCM420 created welds with lower penetration depth, than for FCD600. WM of SCM420 consists mainly of fine grained martensite. Solidification cracks occur in this material under all welding conditions near the weld bottom and thermal axis.

It is possible to create dissimilar metal welds by controlling the C content in the WM by misalignment of the laser beam. In such a way, resulting microstructure and hardness, as well as crack occurrence can be diminished. To create sound welds, to eradicate solidification cracks completely, high minus defocus and full penetration welds can be used. Also using Ni based filler wire is feasible to create sound weld when gap 0.5 mm and higher is used to ensure sufficient Ni content in the WM.

Literature

[1] Fe-Fe3C diagram, Hutni projekt, 1965, Czechoslovakia
[2] ASM Handbook, volume 15, Casting
[3] Pantsar, H., Journal of Laser Applications 16-3, 2004, p. 147-153
[4] ASM Handbook, volume 12, Fractography
[5] Dawes, C., Laser welding, Woodhead Publishing, 1992, p. 147